

Article

A Multi-Analytical Approach for the Characterization of Painting Materials and Metal Soap Formation in Two Artworks by the Argentinian Painter Antonio Berni

Astrid C. Blanco Guerrero^{1,2}, Isabel Alcántara Millán¹, Valeria P. Careaga^{1,2}, Gabriela Siracusano³
and Marta S. Maier^{1,2,3,*}

¹ Departamento de Química Orgánica, Facultad de Ciencias Exactas y Naturales, Universidad de Buenos Aires, Ciudad Autónoma de Buenos Aires C1428EGA, Argentina; astridcbg@gmail.com (A.C.B.G.); isaalcantara23@gmail.com (I.A.M.); pcareaga@qo.fcen.uba.ar (V.P.C.)

² Unidad de Microanálisis y Métodos Físicos en Química Orgánica (UMYMFOR), CONICET—Universidad de Buenos Aires, Ciudad Autónoma de Buenos Aires C1428EGA, Argentina

³ Centro de Investigación en Arte, CONICET, Materia y Cultura, IIAC, Universidad Nacional de Tres de Febrero, Avda. Antártida Argentina 1355, Ciudad Autónoma de Buenos Aires C1104ACA, Argentina; gasiracusano@gmail.com

* Correspondence: maier@qo.fcen.uba.ar

Abstract: This work describes the characterization of pigments and ground layers in two paintings by the renowned Argentinian painter Antonio Berni (1905–1981). The studied paintings are “Toledo” and “Figure” from the collection of the Provincial Museum of Fine Arts in Santa Fe (Argentina). To approach this goal, an integrated investigation comprising in situ X-ray fluorescence measurements by means of a portable system (pXRF), micro-Raman spectroscopy, Attenuated Total Reflection–Fourier transform infrared spectroscopy (ATR-FTIR), and scanning electron microscopy coupled with energy-dispersive X-ray spectroscopy (SEM-EDS) was carried out. The results revealed a chromatic palette with inorganic pigments, such as ultramarine blue, cobalt blue, lead white, zinc white, yellow cadmium, and hydrated chromium oxide (viridian), together with a preparation layer consisting of a mixture of earth, lead white, and calcite in “Toledo”. On the other hand, the preparation layer in “Figure” was characterized as lithopone, a mixture of barium sulfate and zinc sulfide. ATR-FTIR-analysis revealed the formation of metallic soaps in both paintings due to the reaction of fatty acids from a drying oil used as a binder with lead and zinc pigments, as confirmed by comparison with the infrared spectra of synthetic lead and zinc soaps. This study contributes to the understanding of Berni’s painting style and the future restoration of both artworks.

Keywords: inorganic pigments; oil paint; metal salts; pXRF; ATR-FTIR; micro-Raman spectroscopy; SEM-EDS



Citation: Guerrero, A.C.B.; Millán, I.A.; Careaga, V.P.; Siracusano, G.; Maier, M.S. A Multi-Analytical Approach for the Characterization of Painting Materials and Metal Soap Formation in Two Artworks by the Argentinian Painter Antonio Berni. *Minerals* **2023**, *13*, 919. <https://doi.org/10.3390/min13070919>

Academic Editor: José Santiago Pozo Antonio

Received: 16 June 2023

Revised: 30 June 2023

Accepted: 6 July 2023

Published: 8 July 2023



Copyright: © 2023 by the authors. Licensee MDPI, Basel, Switzerland. This article is an open access article distributed under the terms and conditions of the Creative Commons Attribution (CC BY) license (<https://creativecommons.org/licenses/by/4.0/>).

1. Introduction

Antonio Berni (Rosario 1905–Buenos Aires 1981) is one of the most representative artists of Argentine art of the 20th century and a relevant protagonist in the esthetic debates around modernity. In 1925, he received a scholarship from the Jockey Club of Rosario to travel to Europe, settling first in Madrid and then Paris, where he was able to get in contact with the surrealist movement. Back in Argentina by the 1930s, he would encourage new artistic explorations around the idea of a new realism, which was mostly identified with the use of different and unconventional materials and techniques. Since 1935, he represented Argentina in diverse international exhibitions, and was awarded in 1962 at the Venice Biennial [1–4]. All these aspects prompted us to investigate the materiality in his artworks and the development of his painting technique throughout the different artistic phases of his life. In the first stage, we investigated the pictorial materials and supports in two paintings that belong to the collection of the Provincial Museum of Fine Arts Rosa

Galisteo de Rodríguez in the city of Santa Fe (Santa Fe province, Argentina). The painting “Toledo” was painted during his stay in Europe ca. 1928, while “Figure” was painted in 1941 in Buenos Aires. Both artworks were analyzed in a non-invasive manner by portable X-ray fluorescence spectroscopy (pXRF) so as to obtain preliminary information on the elemental composition of the pigments and ground layers.

X-ray fluorescence (XRF) spectroscopy using portable spectrometers is successfully used for the non-destructive and in situ analysis of major and minor elements in cultural heritage objects. It allows rapid access to information on pigments in artworks [5], the composition of metal alloys [6], and the identification of photographic materials [7], among other applications. The ease of use of portable XRF instruments has contributed to the application of the technique by conservators in museums and, in 2020, an excellent workbook on portable XRF for conservators was published [8]. In addition to obtaining elemental information on pictorial materials, this spectroscopic technique can help to select specific areas of artwork for the extraction of micro-samples. In this way, the elemental information obtained by a pXRF analysis of Berni’s paintings aided in the extraction of micro-samples from different areas of “Toledo” and “Figure” that were then analyzed by a combination of analytical techniques for the molecular identification of pigments, grounds, and organic binders. An Attenuated Total Reflection–Fourier transform infrared spectroscopy (ATR-FTIR) analysis allowed for the identification of inorganic and organic components in a non-destructive way and without any preparation of the samples [9]. Scanning electron microscopy coupled with energy-dispersive X-ray spectroscopy (SEM-EDS) and micro-Raman spectroscopy were applied for the characterization of inorganic pigments and ground materials in the layers of the cross-sections of the micro-samples of both paintings.

To date, only two articles have been published on the chemical characterization of pictorial materials in Berni’s paintings. One refers to the artwork “Chacareros” (1935), from which micro-samples were extracted during its restoration and analyzed by SEM-EDS and micro-Raman spectroscopy [10]. The second article comprises conservation studies and a preliminary non-invasive XRF analysis of five paintings of the period 1957–1978 [11].

The two paintings studied in this work by the application of a combination of non-invasive and micro-destructive techniques will allow us to expand our knowledge on the painting materials used by Antonio Berni and address the following points:

- (1) The characterization of the pigments used by Antonio Berni and its comparison to those used by contemporary artists in Argentina.
- (2) The painting technique with a focus on the ground layers.
- (3) The possible degradation processes related to the interaction of pigments and organic binders that could affect the integrity of the artworks.

2. Materials and Methods

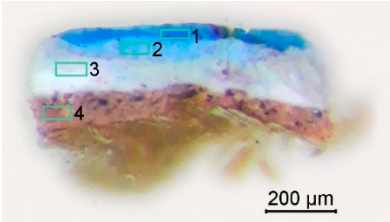
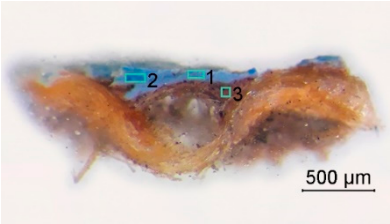
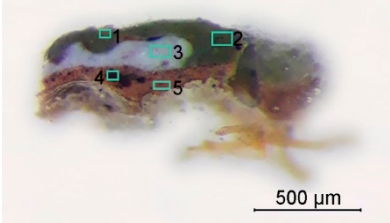
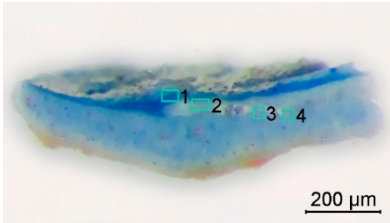
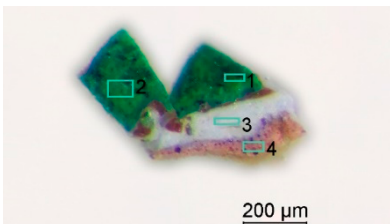
2.1. Analytical Methods

The elemental composition of each color region in both paintings was determined by in situ portable X-ray fluorescence analysis (pXRF) with a Bruker Tracer III-SD portable analyzer. The spectra were registered at 40 kV of voltage and 11 μ A current, with an acquisition time of 100 s with S1PXRF (Bruker) software. The XRF data were analyzed with Artax 7.4.0. (Bruker, Billerica, MA, USA).

Five micro-samples were extracted with a scalpel from the borders of “Toledo” (samples TOL01, TOL02, TOL03, and TOL05) and one (TOL04) from the corner of the front of the painting in order to minimize invasiveness. The description of their color and location in the painting is given in Table 1. For the artwork “Figure”, one fiber with a preparation layer (FIG01) was extracted from the border of the painting. Fragments of samples TOL04, TOL05, and FIG01 were analyzed by ATR-FTIR without previous preparation. Cross-sections were prepared by embedding fragments of the samples (an area of less than 1 mm²) into an acrylic resin Subiton[®] (Buenos Aires, Argentina) and polished with sandpaper decreasing in size (until 12,000 mesh) to obtain the cross-sections. Samples and their cross-sections

were observed and photographed under a Leica MZ6 stereomicroscope equipped with an OMAX USB A3590U camera to obtain information on the pictorial and preparation layers.

Table 1. Elemental composition of the cross-sections of “Toledo” painting samples as determined by SEM-EDS.

Sample and Color	Cross-Section Image	Elemental Composition of Each Layer ¹
TOL01 (blue)		<ol style="list-style-type: none"> 1. <i>Pb, Al, Zn, Si, Co, Ca</i> 2. <i>Pb, Zn, Si, Al, Ca</i> 3. <i>Pb, Zn, Ca</i> 4. <i>Ca, Si, Pb, Fe, Na, Mg</i>
TOL02 (blue)		<ol style="list-style-type: none"> 1. <i>Zn, Si, Al</i> 2. <i>Zn, Pb, Si, Al</i> 3. <i>Pb, Ca, Si, Fe, Al, Zn</i>
TOL03 (dark green)		<ol style="list-style-type: none"> 1. <i>Pb, Al, Cd, Zn, Si, K, Ca, Cr, Fe</i> 2. <i>Si, Al, Cd, Zn, Cr, Pb, Ca, Mg, K</i> 3. <i>Pb, Zn, Ca</i> 4. <i>Ca, Si, Pb, Mg, Al, Fe</i> 5. <i>Pb, Ca, Fe, Si, Al, Na, K</i>
TOL04 (blue)		<ol style="list-style-type: none"> 1. <i>Pb, Zn, Al, Mg, Co, Ca</i> 2. <i>Pb, Zn, Al, Ca</i> 3. <i>Zn, Pb, Si, Al, K, Ca</i> 4. <i>Zn, Al, Fe</i>
TOL05 (green)		<ol style="list-style-type: none"> 1. <i>Cr, Pb, Si, Cd, Zn, Al, K</i> 2. <i>Cr, Pb, Si, Zn, Cd, Al, K</i> 3. <i>Zn, Pb, Si, Al, Ca</i> 4. <i>Si, Pb, Zn, Ca, Fe, Al, Ba, Mg, K</i>

¹ Major elements in each layer are marked in italic style.

Scanning electron microscopy coupled with energy-dispersive X-ray spectroscopy (SEM-EDS) analyses were carried out using an Environmental Scanning Electron Microscope Quanta FEG-250 with an acceleration voltage of 15 kV. Cross-sections of the samples were coated by sputtering with a thin layer of gold in an Edwards S150B sputter coater. Several measurements were carried out on selected areas of the cross-sections of the samples.

The molecular composition of the materials in both paintings was obtained by Attenuated Total Reflection—Fourier transform infrared spectroscopy (ATR-FTIR) analysis using a Nicolet iS50 infrared spectrometer with a diamond single-bounce ATR accessory (Thermo

Fisher Scientific Inc., Waltham, MA, USA). Spectra were acquired in the 4000–400 cm^{-1} spectral range by performing 64 scans at 4 cm^{-1} resolution. The spectrum of air was used as the background. Spectral data were collected with the Omnic v9.2 (Thermo Fisher Scientific Inc., Waltham, MA, USA) software without post-run processing. Data were processed with Origin software version 2021 (OriginLab Corp., Northampton, MA, USA).

Raman spectroscopy measurements in the cross-sections of the samples were recorded on a RenishawInVia spectrometer coupled to a Leica microscope DM2500M with a grating of 1200 lines/mm. The diode laser line at 785 nm was used for excitation and focused on the layers of the cross-sections using a 50 \times objective lens. The wavenumber range of 3200–100 cm^{-1} was recorded in each case with a spectral resolution of 1 cm^{-1} . The laser power was set between 1.5 and 15 mW at the sample. Each spectrum was averaged over 10–20 scans corresponding to a collection time of 20 s. Spectra were analyzed with Omnic v9.0 (Thermo Fisher Scientific Inc., Waltham, MA, USA) software and processed with Origin software version 2021 (OriginLab Corp., Northampton, MA, USA).

2.2. Synthesis of Lead and Zinc Carboxylates

Lead and zinc palmitates were synthesized according to the methods reported by Mazzeo et al. [12]. Lead palmitate was prepared by mixing a 0.02 M solution of lead nitrate ($\text{Pb}(\text{NO}_3)_2$) in a mixture of water:ethanol:methanol (5:5:2) (30 mL) with a 0.02 M solution of palmitic acid in methanol (12.5 mL). The mixture was left for 10 min in an ultrasonic bath. The crystalline solid was filtered, washed subsequently with ethanol and ether, and dried under a vacuum. Zinc palmitate was synthesized by adding drop by drop 3 mL of a 0.3 M aqueous solution of zinc acetate ($\text{Zn}(\text{CH}_3\text{CO}_2)_2$) to a 0.2 M solution of palmitic acid in ethanol (12 mL). The solution was heated at 50 $^\circ\text{C}$ for 3 h. The crystalline solid was filtered, washed subsequently with ethanol and ether, and dried under a vacuum. Lead nitrate was provided by Mays & Baker Ltd., while palmitic acid and zinc acetate were purchased from Sigma-Aldrich. The synthesized palmitates were characterized by ATR-FTIR by comparison to the spectra reported in the literature [12].

3. Results

3.1. “Toledo”

3.1.1. Analysis by Portable X-ray Fluorescence Spectroscopy

The artwork “Toledo” is characterized by a chromatic palette based on ocher, green, and blue color hues. Three green (TL01, TL02, and TL03) and four blue (TL04, TL05, TL06, and TL07) regions of the painting were investigated (Figure 1).



Figure 1. “Toledo” (ca.1928) and analyzed points by pXRF.

The XRF spectra of the green regions (TL01, TL02, and TL03) (Figure 2) showed the presence of lead and zinc peaks as the main elements together with chromium peaks. This composition is consistent with the use of lead white ($2\text{PbCO}_3 \cdot \text{Pb}(\text{OH})_2$) [13] and zinc white (ZnO) [14], while the presence of chromium could be related to a chromium green pigment, such as synthetic chromium oxide (Cr_2O_3) or viridian ($\text{Cr}_2\text{O}_3 \cdot 2\text{H}_2\text{O}$) [15]. Regions TL02 and TL03 revealed a higher content of chromium compared to TL01 together with a low content of iron that could be related to the use of Prussian blue to obtain a green-bluish hue, especially in region TL03, or the ground of the painting.

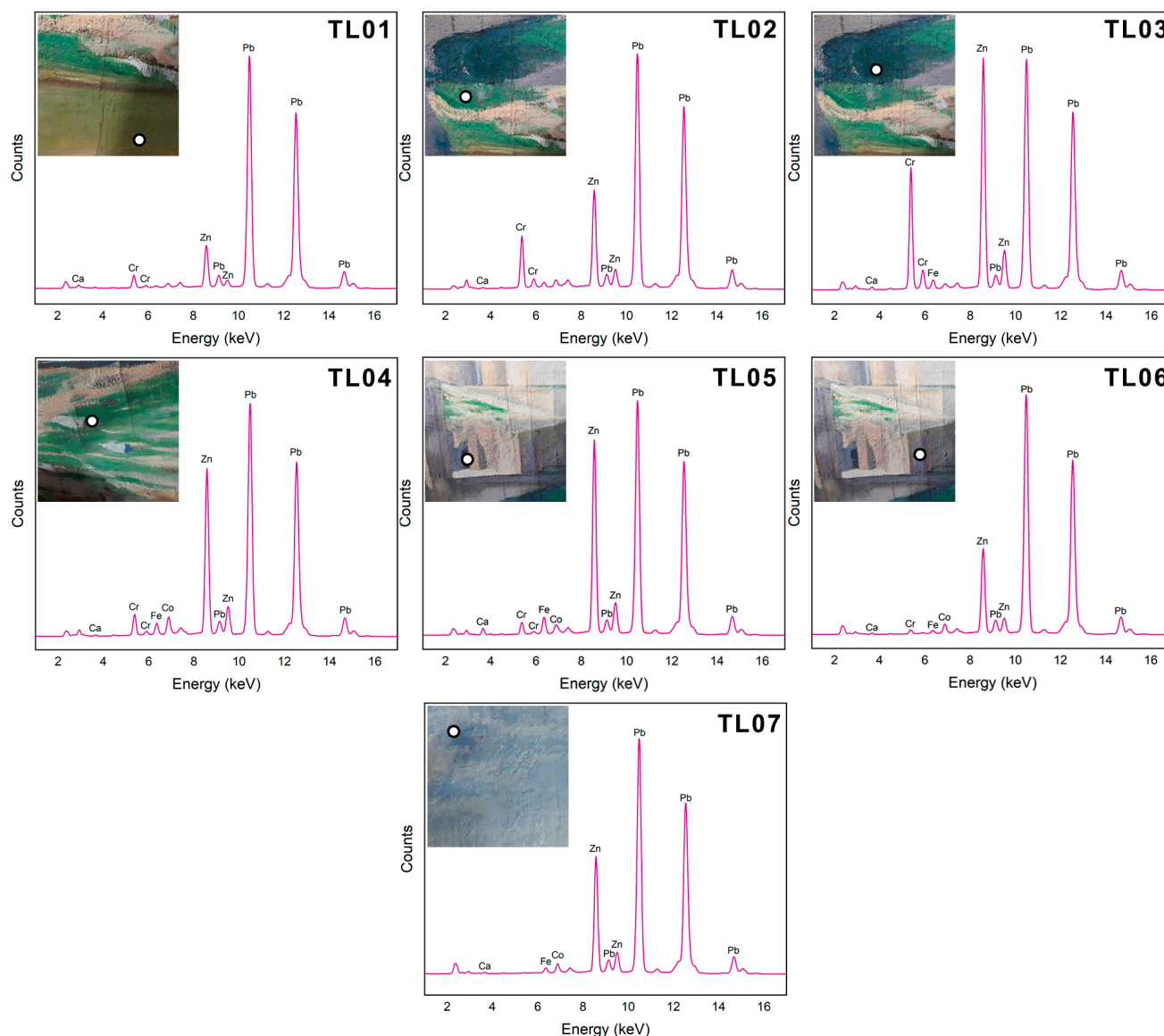


Figure 2. XRF spectra of green (TL01–TL03) and blue (TL04–TL07) regions in the “Toledo” painting.

The XRF spectra of the four blue color regions (TL04, TL05, TL06, and TL07) (Figure 2) revealed, similar to the green areas, the predominance of lead and zinc peaks. The cobalt peak was detected in the four zones and could be ascribed to cobalt blue, a synthetic mixed oxide of cobalt and aluminum oxide ($\text{CoO} \cdot \text{Al}_2\text{O}_3$) [16]. Regions TL04, TL05, and TL06 also showed the presence of chromium that could be related to the use of chromium green in a layer beneath or close to the blue brushstrokes. As for the green regions, iron was detected in the blue zones and could be ascribed to Prussian blue or the ground of the artwork.

Based on the results obtained by pXRF, five micro-samples were extracted from the painting, four from the borders (TOL01, TOL02, TOL03, and TOL05) and one from the front

(TOL04) (Figure 3), in order to characterize the painting palette, the pictorial technique, and eventual deterioration patterns.



Figure 3. Locations of the micro-samples extracted from the “Toledo” (ca.1928) painting.

3.1.2. Analysis of Micro-Samples by SEM-EDS and Micro-Raman Spectroscopy

Table 1 shows the cross-section images of the five samples. With the exception of sample TOL04, the one extracted from the front of the painting, the other four samples depict one, two, or three pictorial layers and a brownish ground layer. Sample TOL02 also shows the fibers of the canvas in the cross-section.

Ground Layer

The elemental composition of the ground layer, as determined by SEM-EDS in samples TOL01, TOL02, TOL03, and TOL05 (Table 1), revealed the presence of lead, calcium, silicon, and iron as major elements together with minor amounts of potassium, aluminum, sodium, and magnesium. The presence of iron in combination with silicon, aluminum, sodium, and magnesium is characteristic of iron earth, which has traditionally been used as a pigment and for the preparation of colored grounds [17].

The Raman spectra of the ground layer in the four samples showed characteristic bands for hematite ($\alpha\text{-Fe}_2\text{O}_3$) at 225, 292, 410, and 611 cm^{-1} [18] in accordance with the presence of this chromophore in red earth, together with a carbonate stretching band at 1050 cm^{-1} , which is typical of lead white ($2\text{PbCO}_3\cdot\text{Pb}(\text{OH})_2$), and a characteristic band of calcite (CaCO_3) at 1086 cm^{-1} [19]. Figure 4a shows the Raman spectrum of the ground layer in sample TLO01.

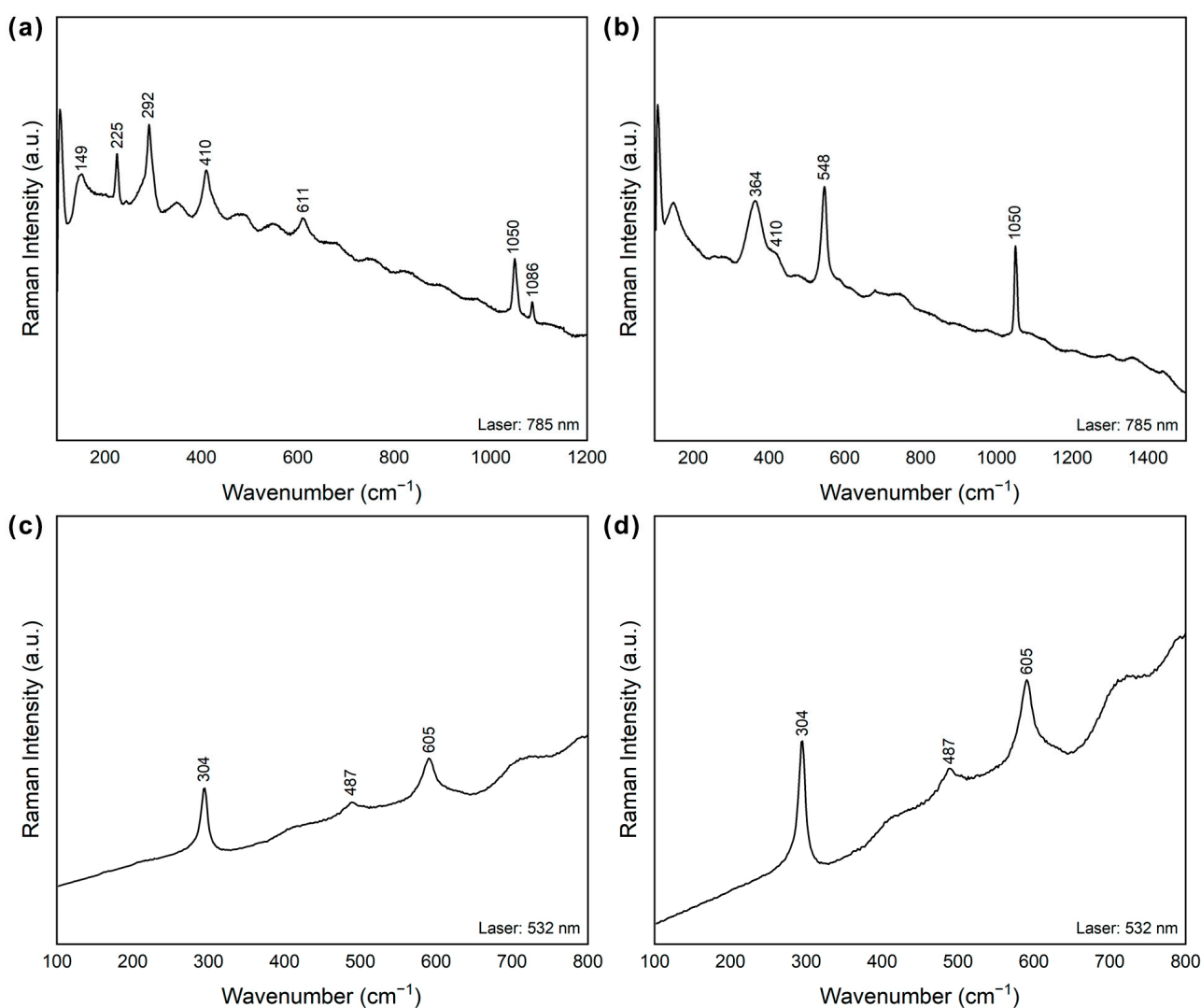


Figure 4. Raman spectra of (a) the ground layer of TLO01, (b) the blue layer of TLO01, (c) the green layer of TOL03, (d) the green layer of TOL05.

Pigment Identification

SEM-EDS analysis of the upper blue layer in the cross-section of sample TOL01 (Table 1) indicated the presence of cobalt, together with aluminum, silicon, lead, and zinc, as major elements. The presence of cobalt could be assigned to cobalt blue, a synthetic pigment composed of cobalt oxide and aluminum oxide with the stoichiometry $\text{CoO}\cdot\text{Al}_2\text{O}_3$ [16].

A micro-Raman spectroscopy analysis of the blue layer of TOL01 revealed peaks at 364 and 548 cm^{-1} , which are characteristic of ultramarine blue [19], and a peak at 1050 cm^{-1} assigned to lead white (Figure 4b). No Raman peaks ascribed to cobalt blue or zinc oxide have been detected. According to the literature, cobalt blue could only be characterized in fresco and casein tempera models by Raman with excitation at 531.5 nm, while laser radiations at 630, 780, and 1064 nm gave no peaks [20,21]. These results can explain the absence of Raman peaks for this pigment in the sample. Nevertheless, the non-invasive identification of cobalt by pXRF analysis in the four regions of the painting (TL04, TL05, TL06, and TL07) and SEM-EDS results in the blue layers of the cross-sections of samples TOL01 and TOL04 pointed to the use of this blue pigment in the painting. Similar to sample TOL01, peaks at 548 cm^{-1} for ultramarine and 1050 cm^{-1} for lead white were identified in the blue layers of samples TOL02 and TOL04 (data not shown). We presume the use of artificial ultramarine blue according to the date of the painting. Since the 19th century, ultramarine was manufactured in France and Germany and became a common pigment used by impressionists and post-impressionists [22]. In the same way, similar to cobalt blue, zinc oxide could not be identified by micro-Raman spectroscopy at 785 nm. This is coincidental with the results of Burrafato et al. [20], who obtained Raman spectra for zinc oxide only when using laser radiations at 532 and 633 nm. Nevertheless, the infrared spectrum of sample TOL04 (Figure 5a) clearly showed a strong band in the range 600–400 cm^{-1} that was assigned to the Zn–O vibration in zinc oxide by comparison to the infrared spectrum of ZnO purchased from Cornelissen (Figure 5b). The spectrum of TOL04 also revealed characteristic bands of oil as binders. The broad band centered at 3365 cm^{-1} was assigned to the O–H stretching vibration typical of oxidation products of oil together with bands at 2919 and 2850 cm^{-1} , which were characteristic of C–H vibrations of methyl and methylene groups [23]. Two weak bands at 1735 and 1706 cm^{-1} were associated with the stretching vibration of the carbonyl groups. The band at 1735 cm^{-1} was assigned to the ester group in acylglycerides, while the band at 1706 cm^{-1} was typical of the carboxyl group in free fatty acids produced by hydrolysis of the ester groups. On the other hand, the strong band at 1535 cm^{-1} suggested the formation of metal soaps by the interaction of the oil with pigments, such as lead white and zinc oxide [12]. In order to confirm the presence of metal soaps in the sample, we synthesized lead and zinc palmitates as references. The infrared spectra of both metal salts differed in the number and position of the carboxylate bands. Lead palmitate showed one sharp band at 1512 cm^{-1} together with a weaker and partially overlapped band at 1538 cm^{-1} (Figure 5c), while zinc palmitate revealed only one band at 1535 cm^{-1} (Figure 5d) [12]. By comparing the infrared spectrum of TOL04 (Figure 5a) with lead and zinc palmitates, we observed a coincidence of the carbonyl peak at 1535 cm^{-1} in TOL04 with zinc palmitate. These results confirmed the presence of zinc soaps in the sample.

The two green samples (TOL03 and TOL05) showed different shades. TOL03 is olive green while TOL05 depicts an intense and bright green color. Both samples revealed the presence of chromium, cadmium, lead, and zinc as major elements by SEM-EDS analyses (Table 1). A micro-Raman spectroscopy analysis of the green layers in the cross-sections of both samples (Figure 4c,d) indicated bands at 304 and 605 cm^{-1} , which are characteristic of cadmium yellow (CdS) [24], and a band at 487 cm^{-1} of hydrated chromium oxide ($\text{Cr}_2\text{O}_3 \cdot 2\text{H}_2\text{O}$), known as viridian [19]. The differences in shades in both green samples might be related to the amount of viridian used in combination with cadmium yellow. In fact, sample TOL03 contains chromium as a minor element in comparison to TOL05 (Table 1). The infrared spectrum of TOL05 (Figure 5e) showed bands at 3533, 1395, 1048, and 679 cm^{-1} ascribed to lead white [25], together with a well-defined band at 1538 cm^{-1} that was assigned to the carboxylate vibration of a zinc salt. The band at 1738 cm^{-1} of a carbonyl ester group is weak in comparison to the carboxylate band. This reflects the degradation of the oil by the formation of metal soaps in the presence of lead and zinc white.

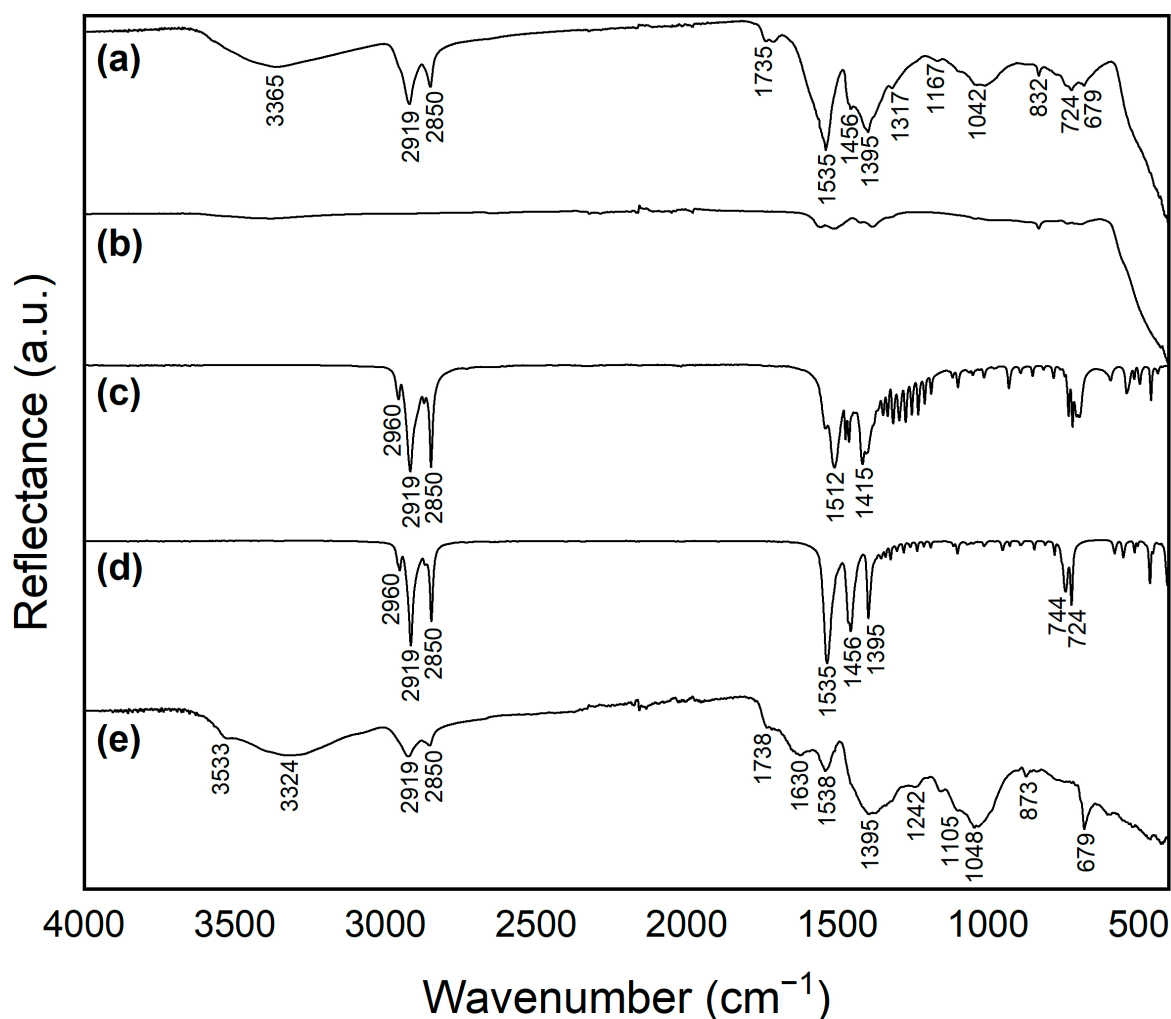


Figure 5. ATR-FTIR spectra of (a) TOL04, (b) ZnO (Cornelissen), (c) synthetic lead palmitate, (d) synthetic zinc palmitate, and (e) TOL05.

Cross-sections of samples TOL01, TOL04, and TOL05 showed a white layer beneath the blue and green pictorial layers. The white layers contain lead and zinc as major elements, as determined by SEM-EDS, while micro-Raman spectroscopy indicated the presence of lead white by bands at 410 and 1050 cm^{-1} . Zinc white could not be detected by this spectroscopic technique using a laser radiation of 785 nm but its presence in samples TOL04 and TOL05 was confirmed by ATR-FTIR, as described before.

3.2. "Figure"

3.2.1. Analysis by Portable X-ray Fluorescence Spectroscopy

Nine regions from the painting (FG01–FG09) were non-invasively analyzed by pXRF (Figure 6).

All the XRF spectra of the painting (Figure 7) showed the presence of zinc and lead peaks as the main elements in accordance with the use of zinc white (ZnO) and lead white ($2\text{PbCO}_3 \cdot \text{Pb}(\text{OH})_2$). The green region (FG01) revealed the presence of chromium, which could be related to viridian, a synthetic hydrated chromium oxide ($\text{Cr}_2\text{O}_3 \cdot 2\text{H}_2\text{O}$) with a brilliant green hue [15]. For the light blue color of the iris of the eye (FG02), cobalt and chromium peaks indicated the use of cobalt blue in combination with green chromium oxide to obtain a blue-greenish hue. The identification of minor barium and sulfur peaks could be related to the presence of barium sulfate, a white compound used as filler or in combination with ZnS in lithopone [26].



Figure 6. “Figure” (1941) and analyzed points by pXRF.

With regard to the flesh tone of the arm (FG03), the spectrum indicated chromium, iron, and lead peaks together with an intense zinc peak. The presence of iron could be related to the use of iron oxide, such as yellow ochre ($\text{Fe}_2\text{O}_3 \cdot n\text{H}_2\text{O}$) and/or red ochre (Fe_2O_3), in combination with lead and zinc white pigments. The identification of chromium may be ascribed to viridian from the layer beneath or to the mixture with chrome yellow (PbCrO_4 or $\text{PbCrO}_4 \cdot \text{PbSO}_4$) or chrome orange ($\text{PbCrO}_4 \cdot \text{Pb}(\text{OH})_2$) to achieve a specific hue of the flesh.

For the red of the lower lip (FG04), the detection of cadmium and selenium indicated cadmium sulfoselenide, a red synthetic pigment prepared from alkaline sulfides and selenides [27]. This pigment was also identified in the cheek of the woman (FG05) together with iron, presumably from an earth pigment, to obtain the desired flesh tone. The use of cadmium red has already been reported in Berni’s painting “Chacareros” [10]. In the border of the blouse sleeve (FG06), the detection of an intense Zn peak together with lead indicated the use of zinc and lead whites. Concerning the background (FG07), the spectrum revealed peaks of chromium and iron together with major peaks of zinc and lead. This composition suggested the use of green and ochre pigments to accomplish a green-yellowish hue. For the black hair with grey details (FG08), the spectrum revealed iron, together with zinc and lead as major peaks. Iron could be ascribed to iron oxide (Fe_3O_4) and was responsible for the black color, but the use of a carbon-based pigment could not be discarded. The detection of calcium with higher intensity as in the other regions of the painting could indicate charcoal [28]. Finally, the spectrum of the brown region of the skirt (FG09) revealed iron, lead, and chromium peaks together with an intense zinc peak. Iron may be related to an earth pigment while chromium may be ascribed to chrome orange ($\text{PbCrO}_4 \cdot \text{Pb}(\text{OH})_2$).

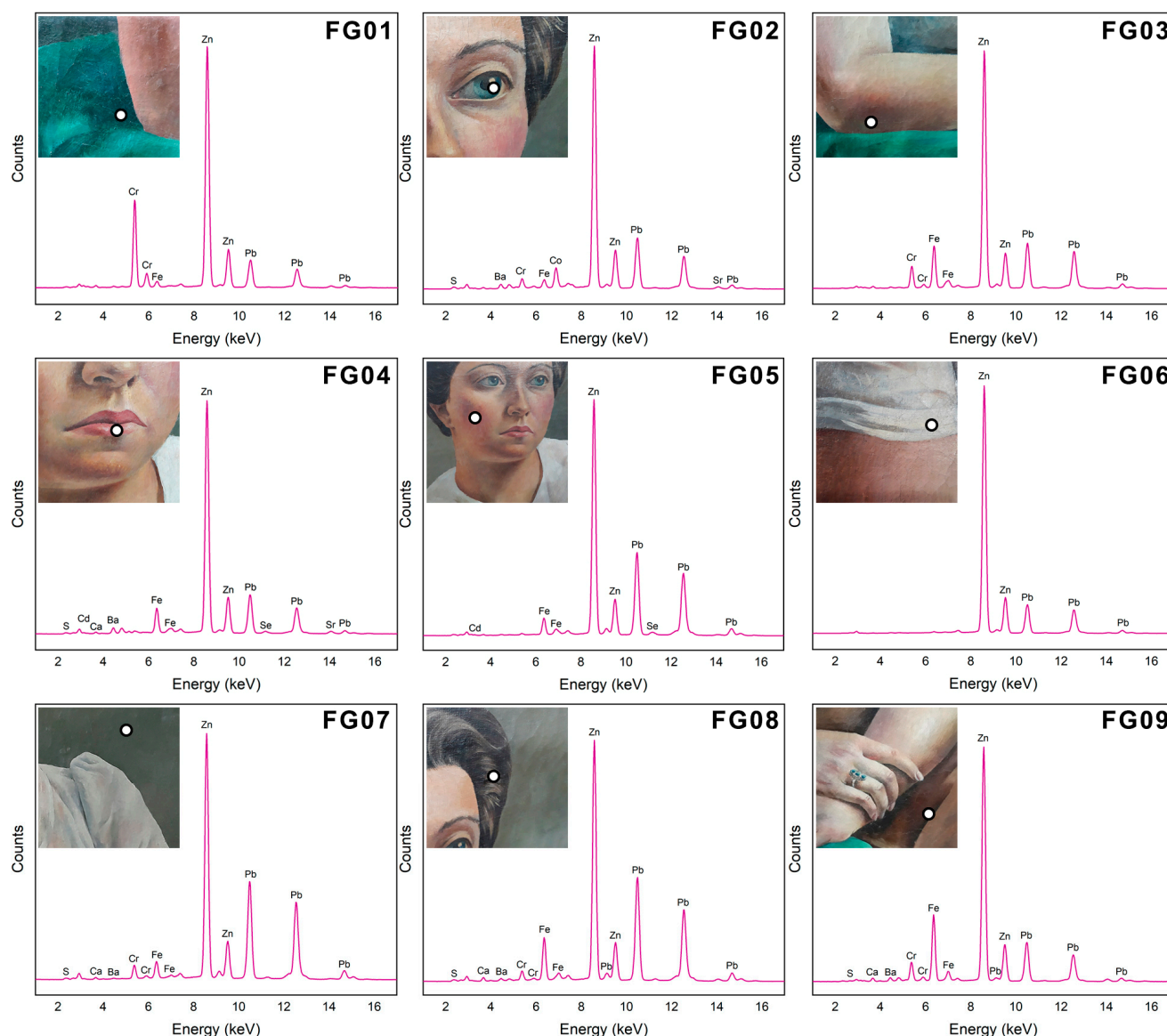


Figure 7. XRF spectra of the nine regions analyzed in the “Figure” painting.

3.2.2. Analysis of the Preparation Layer of the Painting by SEM-EDS, ATR-FTIR, and Micro-Raman Spectroscopy

The detection of barium and sulfur, together with major amounts of zinc in several regions of the painting, prompted us to investigate if lithopone ($\text{ZnS} + \text{BaSO}_4$) had been used as a preparatory layer. Therefore, a sample (FIG01) was extracted from a fiber of the border of the painting (Figure 8a) and divided into two. One portion was included in a resin to obtain the cross-section and analyzed by SEM-EDS and micro-Raman spectroscopy. The other portion of the sample was analyzed with ATR-FTIR.

SEM-EDS analysis of the white region (1) of the cross-section of the sample (Figure 8b) indicated the presence of zinc, sulfur, and barium as major elements, together with low amounts of silicon. Mapping analysis of the four elements showed an even distribution for major barium, sulfur, and zinc (Figure 8c) compatible with lithopone, a mixture of BaSO_4 and ZnO , or a mixture of lithopone and ZnO . In order to determine the presence of lithopone, the cross-section of FIG01 was analyzed by Raman microscopy. The spectrum (Figure 9a) showed a band at 347 cm^{-1} that was assigned to zinc sulfide, while bands at 450 , 458 , 615 , 644 , and 986 cm^{-1} were ascribed to barium sulfate, in accordance with lithopone [18].

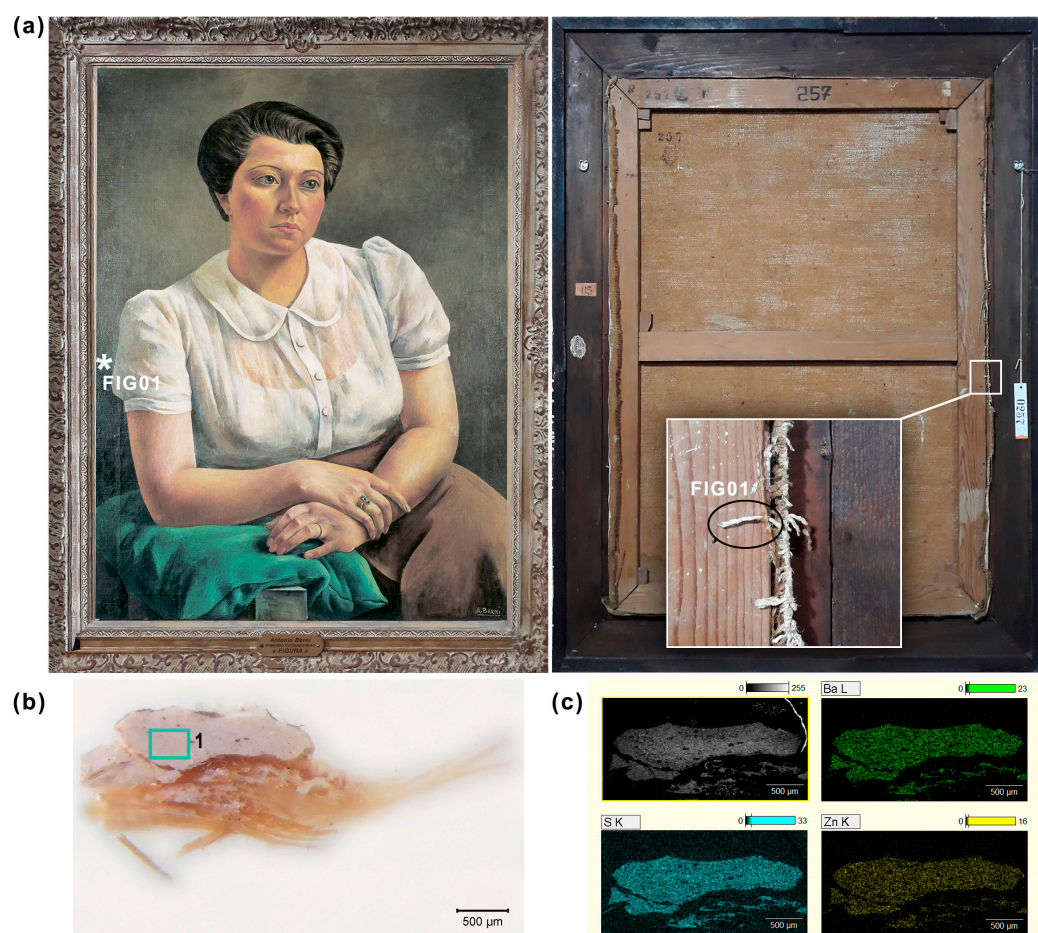


Figure 8. (a) Location of the sample extracted from a fiber of the border of the “Figure” (1941) painting, (b) cross-section of sample FG01, and (c) SEM-EDS mapping analysis of FIG01.

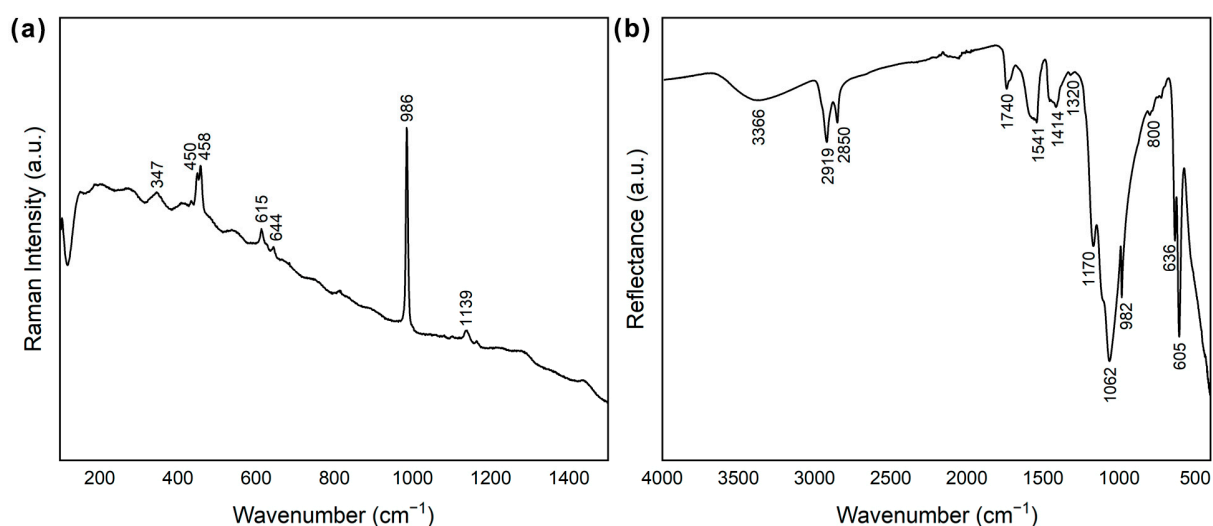


Figure 9. (a) Raman spectrum of the white layer in the cross-section of sample FIG01 and (b) infrared spectrum of sample FIG01.

Non-destructive ATR-FTIR analysis of a portion of the sample (Figure 9b) revealed characteristic bands of BaSO_4 at 1170, 1062, 982, 636, and 605 cm^{-1} [26], as well as a strong band between 600 and 400 cm^{-1} that was assigned to ZnO. The identification of zinc white by infrared analysis was in accordance with the distribution of zinc in the SEM-EDS

mapping of the cross-section of the sample. These results were consistent with the use of a mixture of lithopone and zinc oxide as the ground layer. The infrared spectrum also showed bands at 2919, 2850, and 1740 cm^{-1} , typical of oil as a binder. Similar to Toledo painting, the low intensity of the carbonyl band at 1740 cm^{-1} and the presence of a band at 1541 cm^{-1} ascribed to a zinc salt were indicative of the degradation of the oil binder by the formation of zinc salts.

4. Discussion

The pigments characterized in the “Toledo” and “Figure” paintings revealed a restricted chromatic palette based on the use of inorganic pigments and their mixtures to obtain different color shades. Cobalt blue and synthetic ultramarine blue were Berni’s choice for the blues while viridian, the hydrated chromium oxide, was the green pigment characterized in both paintings. In “Toledo”, viridian was identified together with cadmium yellow, which reflects the intention of the artist to achieve different green shades. For the reds, synthetic cadmium sulfoselenide was identified in “Figure”. These pigments have also been reported for Berni’s painting “Chacareros” (1935) [10] and in paintings of Argentinian artists contemporary to Berni, such as Pío Collivadino (1869–1945) [24] and Benito Quinquela Martín (1890–1977) [29]. This indicates that these pigments were available from local art suppliers in Buenos Aires while synthetic organic pigments, such as blue and green phthalocyanines, were still not marketed in Argentina.

Lead and zinc whites were also characterized in the pictorial layers in both paintings. Titanium whites were not commercialized at that time in Argentina and in Europe; they were available by the end of 1930. As revealed in some of the cross-sections of “Toledo”, Berni not only used zinc white as a pigment but as a preparation layer onto the earth ground, possibly to highlight the color of the painting layers. Zinc oxide mixed with gypsum has been detected as a ground in “Chacareros” [10], while in “Figure”, we characterized the use of lithopone and zinc oxide as a preparation layer. Based on the identification of sulfur, barium, and zinc by XRF analysis, Bondía Fernández et al. [11] suggested the use of a thick layer of lithopone in Berni’s painting “La Casa del Sastre” (1957), presumably as a strategy to economize the painting materials. The identification of zinc oxide as a pigment and preparation layer in the paintings studied so far poses a risk for the structural stability and appearance of these oil artworks due to the formation of zinc soaps that can lead to surface efflorescence and delamination of the paintings [30].

The identification of zinc salts in samples from the “Toledo” and “Figure” artworks is the first report on their presence in Berni’s paintings. This information is essential to address appropriate conservation strategies and improve environmental conditions for their exhibition and storage. This finding enables us to continue studying Berni’s paintings from other periods of his career by focusing on the materials he used, particularly the use of zinc white.

Author Contributions: Conceptualization, M.S.M. and G.S.; methodology, A.C.B.G., I.A.M. and M.S.M.; formal analysis, A.C.B.G., V.P.C. and M.S.M.; investigation, A.C.B.G. and M.S.M.; resources, M.S.M.; data curation, A.C.B.G. and M.S.M.; writing—original draft preparation, M.S.M. and G.S.; writing—review and editing, M.S.M., G.S., A.C.B.G. and V.P.C.; visualization, A.C.B.G. and M.S.M.; supervision, M.S.M.; project administration, M.S.M. and G.S.; funding acquisition, G.S., M.S.M. and V.P.C. All authors have read and agreed to the published version of the manuscript.

Funding: This research was funded by the Agencia Nacional de Promoción Científica y Tecnológica (ANPCyT) (PICT 2015-0440 and PICT 2019-1000), the Consejo Nacional de Investigaciones Científicas y Técnicas (CONICET) (PIP 11220130100288CO and 11220200100811CO), and the University of Buenos Aires (20020170100340BA). V.P.C., G.S. and M.S.M. are Research Members of CONICET.

Data Availability Statement: Not applicable.

Acknowledgments: A.C.B.G. thanks CONICET for a Doctoral Fellowship. I.A.M. thanks ERASMUS+ for a Fellowship. The authors are grateful to M.M. Córdova for the cross-sections of the samples. The authors also acknowledge the Provincial Museum of Fine Arts Rosa Galisteo de Rodríguez and, in special, Laura D’Aloysisio, conservator at the museum at the time when the XRF measurements were performed.

Conflicts of Interest: The authors declare no conflict of interest.

References

1. Nanni, M. Antonio Berni. In *Obra Pictórica 1992–1981*; Museo Nacional de Bellas Artes: Buenos Aires, Argentina, 1984.
2. Pacheco, M.E. *Berni: Escritos y Papeles Privados*; Temas: Buenos Aires, Argentina, 1999.
3. Wechsler, D.B. Imágenes para la resistencia. Intersecciones entre arte y política en la encrucijada de la Internacional Antifascista. Obras y textos de Antonio Berni (1930–1936). In *La Imagen Política*; Medina, C., Ed.; UNAM: Mexico City, Mexico, 2006; pp. 385–412.
4. Wechsler, D. Disputas por lo real. In *AAVV, Arte Moderno Ideas y Conceptos*; Instituto de Cultura-Fundación Mapfre: Madrid, Spain, 2008; pp. 271–313.
5. McGlinchey, C. Handheld XRF for the examination of paintings: Proper use and limitations. In *Handheld XRF for Art and Archaeology*; Shugar, A.N., Mass, J.L., Eds.; Leuven University Press: Leuven, Belgium, 2012; pp. 131–158.
6. Smith, D. Handheld XRF fluorescence analysis of Renaissance bronzes: Practical approaches to quantification and acquisition. In *Handheld XRF for Art and Archaeology*; Shugar, A.N., Mass, J.L., Eds.; Leuven University Press: Leuven, Belgium, 2012; pp. 37–74.
7. Stulik, D.C.; Kaplan, A. Applications of a handheld XRF spectrometer in research and identification of photographs. In *Handheld XRF for Art and Archaeology*; Shugar, A.N., Mass, J.L., Eds.; Leuven University Press: Leuven, Belgium, 2012; pp. 75–130.
8. Bezur, A.; Lee, L.; Loubser, M.; Trentelman, K. *Handheld XRF in Cultural Heritage. A Practical Workbook for Conservators*; The Getty Conservation Institute: Los Angeles, CA, USA, 2020; pp. 1–191.
9. Derrick, M.R.; Stulik, D.; Landry, J.M.K. *Infrared Spectroscopy in Conservation Science*; The Getty Conservation Institute: Los Angeles, CA, USA, 1999; pp. 1–235.
10. Barrio, N.; Marte, F. Estudio material de la obra “Chacareros” de Antonio Berni. Problemáticas de un soporte atípico. *Ge-conservacion* **2010**, *1*, 235–257. [[CrossRef](#)]
11. Bondía Fernández, C.; Hortal Valverde, L.; Illán Gutiérrez, A.; Romero Asenjo, R. Aspectos constructivos de la técnica pictórica de Antonio Berni. Consideraciones sobre la conservación de su obra. *Conserv. De Arte Contemp. 15ª Jorn.* **2014**, *2014*, 185–203.
12. Mazzeo, R.; Prati, S.; Quaranta, M.; Joseph, E.; Kendix, E.; Galeotti, M. Attenuated total reflection micro FTIR characterization of pigment–binder interaction in reconstructed paint films. *Anal. Bioanal. Chem.* **2008**, *392*, 65–76. [[CrossRef](#)] [[PubMed](#)]
13. Gettens, R.J.; Kühn, H.; Chase, W.T. Lead white. In *Artists’ Pigments. A Handbook of Their History and Characteristics*; Roy, A., Ed.; National Gallery of Art: Washington, DC, USA, 1993; Volume 2, pp. 67–81.
14. Kühn, H. Zinc White. In *Artists’ Pigments. A Handbook of Their History and Characteristics*; Feller, R.L., Ed.; National Gallery of Art: Washington, DC, USA, 1986; Volume 1, pp. 169–186.
15. Newman, R. Chromium Oxide Greens. Chromium Oxide and Hydrated Chromium Oxide. In *Artists’ Pigments. A Handbook of Their History and Characteristics*; West FitzHugh, E., Ed.; National Gallery of Art: Washington, DC, USA, 1997; Volume 3, pp. 273–293.
16. Roy, A. Cobalt Blue. In *Artists’ Pigments. A Handbook of Their History and Characteristics*; Berrie, B.H., Ed.; Archetype Publications: London, UK, 2007; Volume 4, pp. 151–177.
17. Helwig, K. Iron Oxide Pigments. In *Artists’ Pigments. A Handbook of Their History and Characteristics*; Berrie, B.H., Ed.; Archetype Publications: London, UK, 2007; Volume 4, pp. 39–109.
18. Bell, I.M.; Clark, R.J.H.; Gibbs, P.J. Raman spectroscopic library of natural and synthetic pigments (pre-1850 AD). *Spectrochim. Acta A* **1997**, *53*, 2159–2179. [[CrossRef](#)]
19. Caggiani, M.C.; Cosentino, A.; Mangone, A. Pigments Checker version 3.0, a handy set for conservation scientists: A free online Raman spectra database. *Microchem. J.* **2016**, *129*, 123–132. [[CrossRef](#)]
20. Burrafato, G.; Calabrese, M.; Cosentino, A.; Gueli, A.M.; Troja, S.O.; Zuccarello, A. ColoRaman Project: Raman and fluorescence spectroscopy of oil, tempera and fresco paint pigments. *J. Raman Spectrosc.* **2004**, *35*, 879–886. [[CrossRef](#)]
21. Burgio, L.; Clark, R.J.H. Library of FT-Raman spectra of pigments, minerals, pigment media and varnishes, and supplement to existing library of Raman spectra of pigments with visible excitation. *Spectrochim. Acta A* **2001**, *57*, 1491–1521. [[CrossRef](#)]
22. Plesters, J. Ultramarine Blue, Natural and Artificial. In *Artists’ Pigments. A Handbook of Their History and Characteristics*; Roy, A., Ed.; National Gallery of Art: Washington, DC, USA, 1993; Volume 2, pp. 37–65.
23. Lazzari, M.; Chiantore, O. Drying and oxidative degradation of linseed oil. *Polym. Degrad. Stab.* **1999**, *65*, 303–313. [[CrossRef](#)]
24. Buscaglia, M.B.; Halac, E.B.; Reinoso, M.; Marte, F. The palette of Pio Collivadino (1865–1945) throughout his career. *J. Cult. Her.* **2020**, *44*, 27–37. [[CrossRef](#)]
25. Pięta, E.; Olszewska-Świątlik, J.; Paluszkiwicz, C.; Zając, A.; Kwiatek, W.M. Application of ATR-FTIR mapping to identification and distribution of pigments, binders and degradation products in a 17th century painting. *Vib. Spectrosc.* **2019**, *103*, 102928. [[CrossRef](#)]

26. Feller, R.L. (Ed.) Barium Sulfate-Natural and Synthetic. In *Artists' Pigments. A Handbook of Their History and Characteristics*, 1st ed.; National Gallery of Art: Washington, DC, USA, 1986; Volume 1, pp. 47–64.
27. Fiedler, I.; Bayard, M.A. Cadmium yellows, oranges and red. In *Artists' Pigments. A Handbook of Their History and Characteristics*, 1st ed.; Feller, R.L., Ed.; National Gallery of Art: Washington, DC, USA, 1986; Volume 1, pp. 65–108.
28. Tomasini, E.; Siracusano, G.; Maier, M.S. Spectroscopic, morphological and chemical characterization of historic pigments based on carbon. Paths for the identification of an artistic pigment. *Microchem. J.* **2012**, *102*, 28–37. [[CrossRef](#)]
29. Halac, E.B.; Reinoso, M.; Luda, M.; Marte, F. Raman mapping analysis of pigments from *Proas Iluminadas* by Quinquela Martín. *J. Cult. Herit.* **2012**, *13*, 469–473. [[CrossRef](#)]
30. Noble, P. A brief history of metal soaps in paintings from a conservation perspective. In *Metal Soaps in Art Conservation and Research*; Casadio, F., Keune, K., Noble, P., Van Loon, A., Hendriks, E., Centeno, S., Osmond, G., Eds.; Springer Nature Switzerland AG: Cham, Switzerland, 2019; pp. 1–22.

Disclaimer/Publisher's Note: The statements, opinions and data contained in all publications are solely those of the individual author(s) and contributor(s) and not of MDPI and/or the editor(s). MDPI and/or the editor(s) disclaim responsibility for any injury to people or property resulting from any ideas, methods, instructions or products referred to in the content.